Appl. Math. Mech. -Engl. Ed., 2008, **29**(8):975–984
DOI 10.1007/s10483-008-0801-y

Applied Mathematics and Mechanics (English Edition)

Floquet instability of a large density ratio liquid-gas coaxial jet with periodic fluctuation *

LI Zhen (李振), HU Guo-hui (胡国辉), ZHOU Zhe-wei (周哲玮)

(Shanghai Institute of Applied Mathematics and Mechanics,
Shanghai Key Laboratory of Mechanics in Energy and Environment Engineering,
Shanghai University, Shanghai 200072, P. R. China)

(Contributed by ZHOU Zhe-wei)

Abstract By numerical simulation of basic flow, this paper extends Floquet stability analysis of interfacial flow with periodic fluctuation into large density ratio range. Stability of a liquid aluminum jet in a coaxial nitrogen stream with velocity fluctuation is investigated by Chebyshev collocation method and the Floquet theory. Parametric resonance of the jet and the influences of different physical parameters on the instability are discussed. The results show qualitative agreement with the available experimental data.

Key words jet stability, Chebyshev collocation, Floquet theory, parametric resonance, large density ratio

Chinese Library Classification O358
2000 Mathematics Subject Classification 76E17

Introduction

Plateau[1] observed that a cylindrical liquid jet tends to break up into segments of equal length which is nine times the jet radius. Neglecting the effects of gravity and ambient gas, Rayleigh[2] showed that the origin of the jet breakup is the hydrodynamic instability. He indicated that the fastest growing disturbances had a wavelength equaling nine times the jet radius. Weber[3] and Chandrasekhar[4] found that the liquid viscosity has stabilizing effects of reducing the breakup rate and increasing the drop size. Keller, Rubinow and Tu[5] analysed the spatially amplifying capillary waves by transforming Rayleigh's dispersion relation to a moving jet and keeping the frequency real while allowing the wavenumber to be complex. They found that the temporal and spatial growth rates only agree in the infinite Weber number limit. Previous studies[6−8] found that jet breakup has two distinctively different modes of instability. One is the Rayleigh-mode instability due to capillary force in low-speed jets and the other is the Taylor-mode instability due to interfacial pressure and shear in high-speed jets. The Rayleigh-mode instability leads to the breakup of the liquid jet into drops of diameter comparable to the nozzle diameter, while the Taylor-mode instability leads the jet to break up into droplets of diameter much smaller than the nozzle diameter, which is also called atomization. There are experimental results[9−11] available showed that the atomized gas with velocity fluctuation of high frequency is helpful to produce smaller droplets and narrower size distribution, resulting

* Received Jul. 7, 2008
Project supported by the National Natural Science Foundation of China (No. 10772107) and the Program of Science and Technology Commission of Shanghai Municipality of China (No. 071605102)
Corresponding author ZHOU Zhe-wei, Professor, E-mail: zhwzhou@yc.shu.edu.cn

in products with higher quality. So, it is worthwhile to investigate the stability of the jet with velocity fluctuation.

There are not much results of liquid-gas jet with velocity fluctuation, especially for viscous fluid. When investigating the parametric resonance of inviscid liquid - gas jet with pulsation, Zhou and Tang[12] obtained Mathieu Equation and discussed the stable and unstable regions. Wang, Hu and Zhou[13] examined the stability of two-layer flow with periodic fluctuation in a pipe, and discussed the influences of different physical parameters on stability. Woods, Lin[14] and Burya et al.[15] studied liquid film flow over a vibrating inclined plane. However, the previous researchers neglected the effect of viscosity of fluid and seldom studied the cases involving high density ratio and velocity fluctuation. But there are many applications of large density ratio liquid - gas jet, for example, in Spray Forming, the density ratio of liquid metal to gas ranges from 2 000 to 10 000, bringing difficulties to stability analysis. The primary purpose of this paper is to extend Wang Yanxia et al.'s work[13] into large density ratio range to investigate the stability of a coaxial viscous liquid - gas jet with velocity fluctuation.

1 Formulation

A cylindrical viscous liquid jet discharged from a nozzle into a coaxial viscous gas stream, both with velocity fluctuation, as shown in Fig. 1. The two fluids are assumed to be incompressible.

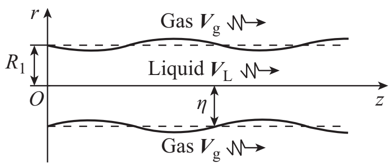

Fig. 1 Coaxial viscous liquid-gas jet with periodic velocity fluctuation

Impose a small disturbance on the basic flow $\bar{V}$ we have $V_i = \bar{V}_i + V_i', i = 1, 2$ the subscript 1 stands for liquid and 2 for gas. Substituting it into the governing equations and boundary conditions and linearizing the system with respect to the disturbance, and utilizing the normal mode method, we can obtain like Wang Yanxia et al.[13] equations in terms of disturbance stream function as follows:

$$\frac{\partial}{\partial t}(E^2\varphi_1) = \frac{1}{Re}E^2E^2\varphi_1 - \mathrm{i}k\bar{V}_1E^2\varphi_1 + \mathrm{i}k\left(\frac{\partial^2\bar{V}_1}{\partial r^2} - \frac{1}{r}\frac{\partial\bar{V}_1}{\partial r}\right)\varphi_1, \tag{1}$$

$$\frac{\partial}{\partial t}(E^2\varphi_2) = \frac{1}{Re}\frac{N}{Q}E^2E^2\varphi_2 - \mathrm{i}k\bar{V}_2E^2\varphi_2 + \mathrm{i}k\left(\frac{\partial^2\bar{V}_2}{\partial r^2} - \frac{1}{r}\frac{\partial\bar{V}_2}{\partial r}\right)\varphi_2, \tag{2}$$

$$E^2 = \frac{\partial^2}{\partial r^2} - \frac{1}{r}\frac{\partial}{\partial r} - k^2,$$

where

$$E^2E^2 = \frac{\partial^4}{\partial r^4} - \frac{2}{r}\frac{\partial^3}{\partial r^3} + \left(\frac{3}{r^2} - 2k^2\right)\frac{\partial^2}{\partial r^2} + \left(\frac{2k^2}{r} - \frac{3}{r^3}\right)\frac{\partial}{\partial r} + k^4.$$

The dimensionless quantities above are Reynolds number $Re = \frac{\rho_1 W_0 R_1}{\mu_1}$, Froude number $Fr = \frac{W_0^2}{gR_1}$, Weber number $We = \frac{\sigma}{\rho_1 W_0^2 R_1}$, density ratio of gas to liquid $Q = \frac{\rho_2}{\rho_1}$, the ratio of Reynolds number to Froude number $R = \frac{Re}{Fr}$, the ratio of dynamic viscosity of gas to liquid $N = \frac{\mu_2}{\mu_1}$ respectively. Here μ is the dynamic viscosity, ρ is the density, and g is the gravitational acceleration in negative z-direction.

Boundary conditions at axis and interface are given as follows:

1) At axis $r = 0$, the axisymmetric boundary conditions:

$$\varphi_1 = \frac{\partial\varphi_1}{\partial r} = 0. \tag{3}$$

2) On the gas-liquid interface $r = 1$, the stream function satisfies:

kinematic condition

$$\frac{\partial \eta}{\partial t} = \mathrm{i}k\varphi_1 - \mathrm{i}k\bar{V}_1 \cdot \eta; \tag{4}$$

shear velocity continuity

$$\frac{\partial \varphi_1}{\partial r} - \frac{\partial \varphi_2}{\partial r} - \left(\frac{\partial \bar{V}_1}{\partial r} - \frac{\partial \bar{V}_2}{\partial r}\right) \cdot \eta = 0; \tag{5}$$

normal velocity continuity

$$\varphi_1 - \varphi_2 = 0; \tag{6}$$

shear stress balance

$$\left(\frac{\partial^2}{\partial r^2} - \frac{\partial}{\partial r} + k^2\right)\varphi_1 - N\left(\frac{\partial^2}{\partial r^2} - \frac{\partial}{\partial r} + k^2\right)\varphi_2 - \left(\frac{\partial^2 \bar{V}_1}{\partial r^2} - \frac{\partial^2 \bar{V}_2}{\partial r^2}\right) \cdot \eta = 0; \tag{7}$$

normal stress balance

$$\begin{aligned} &\frac{\partial}{\partial t}\left(\frac{\partial \varphi_1}{\partial r} - Q\frac{\partial \varphi_2}{\partial r}\right) \\ =& \frac{1}{Re}\left(\frac{\partial^3}{\partial r^3} - \frac{\partial^2}{\partial r^2} + (1-3k^2)\frac{\partial}{\partial r}\right)\varphi_1 - \mathrm{i}k\bar{V}_1\frac{\partial \varphi_1}{\partial r} + \left(\frac{2k^2}{Re} + \mathrm{i}k\frac{\partial \bar{V}_1}{\partial r}\right)\varphi_1 \\ &- \frac{N}{Re}\left(\frac{\partial^3}{\partial r^3} - \frac{\partial^2}{\partial r^2} + (1-3k^2)\frac{\partial}{\partial r}\right)\varphi_2 + \mathrm{i}kQ\bar{V}_1\frac{\partial \varphi_2}{\partial r} - \left(\frac{2k^2}{Re}N + \mathrm{i}kQ\frac{\partial \bar{V}_2}{\partial r}\right)\varphi_2. \end{aligned} \tag{8}$$

3) At gas stream outer boundary $r = \frac{R_2}{R_1} = R_{\max}$,

$$\varphi_2 = 0, \quad \frac{\partial \varphi_2}{\partial r} - R_{\max} \cdot \frac{\partial^2 \varphi_2}{\partial r^2} = 0. \tag{9}$$

2 Basic flow

Since the periodic velocity fluctuation are considered, the basic flows can be written as $\boldsymbol{U}_i = (0, 0, \bar{V}_i(r,t))$, in which the axial velocity $\bar{V}_i(r,t) = \bar{Z}_i(r) + \bar{W}_i(r,t)$, $i = 1, 2$, and $\bar{Z}_i(r)$ and $\bar{W}_i(r,t)$ are the steady and the unsteady part of axial velocity components respectively.

If the pressure gradients are assumed to be constant and $\frac{dP_2/dz}{dP_1/dz} = \beta$[16], the exact solutions of steady part of basic flow can be obtained as

$$\bar{Z}_1 = \frac{R(L^2-1)(\beta-Q)}{4(1-\beta+\beta L^2)}r^2 + \frac{W_{10}}{W_0}, \quad 0 \le r \le 1;$$

$$\bar{Z}_2 = \begin{cases} \dfrac{R(\beta-Q)}{4N(1-\beta+\beta L^2)}(r^2-L^2) + \dfrac{R(\beta-Q)L^2}{2N(1-\beta+\beta L^2)}\ln\left(\dfrac{r}{L}\right) + 1 + \dfrac{W_{10}}{W_0}, & 1 \le r \le L, \\ 1 + \dfrac{W_{10}}{W_0}, \quad r \ge L; \end{cases}$$

where W_{10} is the magnitude of the jet velocity on the z-axis, W_0 is the relative velocity between gas and liquid. L is the thickness of shear layer which is determined by interfacial condition $Z_1(1) = Z_2(1)$. The relations between L and β was discussed in detail by Li Xiaojun et al[16].

The governing equations and boundary conditions of the unsteady part of basic flow are

$$\begin{cases} \dfrac{1}{Re}\left(\dfrac{\partial^2 \bar{W}_1(r,t)}{\partial r^2} + \dfrac{1}{r}\dfrac{\partial \bar{W}_1(r,t)}{\partial r}\right) = \dfrac{\partial \bar{W}_1(r,t)}{\partial t} + \dfrac{\partial \bar{p}_1(z,t)}{\partial z}, \\ \dfrac{N}{Q}\dfrac{1}{Re}\left(\dfrac{\partial^2 \bar{W}_2(r,t)}{\partial r^2} + \dfrac{1}{r}\dfrac{\partial \bar{W}_2(r,t)}{\partial r}\right) = \dfrac{\partial \bar{W}_2(r,t)}{\partial t} + \dfrac{1}{Q}\dfrac{\partial \bar{p}_2(z,t)}{\partial z}; \end{cases} \tag{10}$$

$$\bar{W}_1(1,t) = \bar{W}_2(1,t), \quad r = 1; \tag{11}$$

$$\frac{\partial \bar{W}_1(1,t)}{\partial r} = N \cdot \frac{\partial \bar{W}_2(1,t)}{\partial r}, \quad r = 1; \tag{12}$$

$$\frac{\partial \bar{W}_2(\infty,t)}{\partial r} = 0, \quad r \to \infty. \tag{13}$$

If the frequency of the periodic fluctuation is ω, according to the interfacial condition $\bar{p}_1(z,t) - \bar{p}_2(z,t) = We$, the pressure in unsteady flow can be written as

$$\begin{cases} \bar{p}_1(z,t) = C \cdot \mathrm{e}^{\mathrm{i}\omega t} \cdot z + We, \\ \bar{p}_2(z,t) = C \cdot \mathrm{e}^{\mathrm{i}\omega t} \cdot z, \end{cases}$$

where C is a complex coefficient[13], and define the real of $Wc = -C/(\omega \cdot Q)$ as amplitude factor of the fluctuating velocity. Let the velocity of unsteady flow $\bar{W}_i(r,t) = V_i(r)\mathrm{e}^{\mathrm{i}\omega t}$, we can obtain the exact solution of (10)–(13) represented by Bessel functions[13]. When the variable of Bessel function is very large or very small, the velocity of unsteady flow calculated from the exact solution is inaccurate. This leads to difficulties in the stability analysis of large density ratio liquid-gas jet. In the present paper, the Chebyshev collocation method is used to solve the equations (10)–(13).

Nonlinear transformations are applied to map the physical space to computational space in order to improve the computational efficiency and accuracy. The nonlinear transformations on the inner liquid flow and outer gas flow are

$$r_1 = 1 + \frac{A(y_1 - 1)}{y_1 + 2A + 1}, \quad r_2 = 1 + \frac{A_1(y_2 - 1)}{A_2 - y_2}, \tag{14}$$

in which $A_2 = -1\frac{2A_1}{R_{\max}-1}$, A and A_1 are adjustable parameters. The transformations tend to be linear if A and A_1 become large. For smaller A and A_1, there will be more collocation points distributed within the shear layer at gas-liquid interface.

Then, $V_i(r)$ can be expanded by Chebyshev polynomials as $V_i(r) = \sum\limits_{k=0}^{N} V_i(r_k)\psi_k(r)$, in which $\psi_k(r)|_{k=0}^{N}$ are Lagrangian cardinal functions with Gauss-Lobatto collocation points. Then the differential coefficient on $V_i(r)$ can be written as $\frac{d^m}{dr^m}V_i(r_j) = \sum_{k=0}^{N} V_i(r_k)(D_m)_{jk}$, thus we can solve the equations (10)–(13) and obtain numerical solution of unsteady flow.

3 Chebyshev collocation method

Chebyshev collocation method[17] with Gauss-Lobatto collocation points and the nonlinear coordinates transformations (14) are used to solve the governing equations (1)–(9). We can obtain the equations as follows:

$$\begin{cases} \dfrac{d}{dt}(E_1^2\varphi_{1j}) = \dfrac{1}{Re}E_1^2E_1^2\varphi_{1j} - \mathrm{i}k\bar{V}_1(r,t)|_j E_1^2\varphi_{1j} \\ \qquad + \mathrm{i}k\left(\dfrac{d^2\bar{V}_1(r,t)}{dr^2}\Big|_j - \dfrac{2}{\left(1+\frac{\tanh(\delta y_{ij})}{\tanh(\delta)}\right)}\dfrac{d\bar{V}_1(r,t)}{dr}\Big|_j\right)\varphi_{1j}, \\ \dfrac{d}{dt}(E_2^2\varphi_{2l}) = \dfrac{1}{Re}\dfrac{N}{Q}E_2^2E_2^2\varphi_{2l} - \mathrm{i}k\bar{V}_2(r,t)|_j E_2^2\varphi_{2l} \\ \qquad + \mathrm{i}k\left(\dfrac{d^2\bar{V}_2(r,t)}{dr^2}\Big|_l - \dfrac{1}{\left(1+\frac{A_1(y_{2l}-1)}{A_2-y_{2l}}\right)}\dfrac{d\bar{V}_2(r,t)}{dr}\Big|_l\right)\varphi_{2l}, \end{cases} \tag{15}$$

$$E_i^2 = \frac{d^2}{dr_i^2} - \frac{1}{r_i}\frac{d}{dr_i} - k^2\boldsymbol{I}_i,$$

where

$$E_i^2 E_i^2 = \frac{d^4}{dr_i^4} - \frac{2}{r_i}\frac{d^3}{dr_i^3} + \left(\frac{3}{r_i^2} - 2k^2\right)\frac{d^3}{dr_i^3} + \left(\frac{2k^2}{r_i} - \frac{3}{r_i^3}\right)\frac{d}{dr_i} + k^4 \boldsymbol{I}_i, \quad i = 1, 2.$$

M_1 and M_2 are the numbers of the collocation points in the liquid and the gas region respectively, and $\boldsymbol{I}_1$ and $\boldsymbol{I}_2$ are identity matrix of M_1 and M_2 dimensions respectively. The boundary and the interfacial conditions are:

1) At axis $y_1 = -1$, the axisymmetric boundary conditions:

$$\varphi_{1M_l} = \left.\frac{d\varphi_{1j}}{dr_1}\right|_{M_1 j} = 0. \tag{16}$$

2) On the gas-liquid interface $y_1 = y_2 = 1$, the following conditions are satisfied:
kinematic condition

$$\left.\frac{dh}{dt}\right|_1 = \mathrm{i}k\varphi_{11} - \mathrm{i}k\bar{V}_1(r,t)h|_1; \tag{17}$$

shear velocity continuity

$$\varphi_{11} - \varphi_{21} = 0; \tag{18}$$

normal velocity continuity

$$\left.\frac{d\varphi_{1j}}{dr_1}\right|_{1j} - \left.\frac{d\varphi_{2l}}{dr_2}\right|_{1l} - \left(\left.\frac{d\bar{V}_1(r,t)}{dr}\right|_1 - \left.\frac{d\bar{V}_2(r,t)}{dr}\right|_1\right) h|_1 = 0; \tag{19}$$

shear stress balance

$$\begin{aligned}&\left(\left.\frac{d^2\varphi_{1j}}{dr_1^2}\right|_{1j} - \left.\frac{d\varphi_{1j}}{dr_1}\right|_{1j}\right) + k^2\varphi_{11} - N\left[\left(\left.\frac{d^2\varphi_{2l}}{dr_2^2}\right|_{1l} - \left.\frac{d\varphi_{2l}}{dr_2}\right|_{1l}\right) + k^2\varphi_{21}\right]\\ &- \left(\left.\frac{d^2\bar{V}_1(r,t)}{dr^2}\right|_1 - \left.\frac{Nd^2\bar{V}_2(r,t)}{dr^2}\right|_1\right) h|_1 = 0;\end{aligned} \tag{20}$$

normal stress balance

$$\begin{aligned}&\frac{d}{dt}\left(\left.\frac{d^2\varphi_{1j}}{dr_1}\right|_{1j} - Q\left.\frac{d\varphi_{2l}}{dr_2}\right|_{1l}\right)\\ =&\frac{1}{Re}\left(\left.\frac{d^3\varphi_{1j}}{dr_1^3}\right|_{1j} - \left.\frac{d^2\varphi_{1j}}{dr_1^2}\right|_{1j} + (1-3k^2)\left.\frac{d^2\varphi_{1j}}{dr_1}\right|_{1j}\right) - \mathrm{i}k\bar{V}_1(r,t)|_1\left.\frac{d\varphi_{1j}}{dr_1}\right|_{1j}\\ &+ \left(\frac{2k^2}{Re} + \mathrm{i}k\left.\frac{d\bar{V}_1(r,t)}{dr}\right|_1\right)\varphi_{11} - \frac{N}{Re}\left(\left.\frac{d^3\varphi_{2l}}{dr_2^3}\right|_{1l} - \left.\frac{d^2\varphi_{2l}}{dr_2^2}\right|_{1l} + (1-3k^2)\left.\frac{d^2\varphi_{2l}}{dr_2}\right|_{1l}\right)\\ &+ \mathrm{i}kQ\bar{V}_2(r,t)|_1\left.\frac{d\varphi_{2l}}{dr_2}\right|_{1l} - \left(\frac{2k^2}{Re}N + \mathrm{i}kQ\left.\frac{d\bar{V}_2(r,t)}{dr}\right|_1\right)\varphi_{21} - \mathrm{i}k(1-k^2)Weh|_1.\end{aligned} \tag{21}$$

3) At gas stream boundary $y_2 = -1$,

$$\varphi_{2M_2} = 0, \quad \left.\left(\frac{d\varphi_{2l}}{dr_2} - R_{\max}\cdot\frac{d^2\varphi_{2l}}{dr_2^2}\right)\right|_{M_2 l} = 0. \tag{22}$$

Using the Lanczos method, eight equations in (15) are replaced by eight boundary conditions (16), (18)–(22). The interfacial function is an additional unknown variable, which can be solved by equation (17).

Then we obtain a system of ordinary differential equations with $M_1 + M_2 + 1$ unknowns $\varphi_{11}, \varphi_{12}, \cdots, \varphi_{1M_1}; \varphi_{21}, \varphi_{22}, \cdots, \varphi_{2M_2}; h$:

$$\boldsymbol{M}\frac{\partial \varphi}{\partial t} = [\boldsymbol{B} + \boldsymbol{C}\cdot\cos(\omega t) + \boldsymbol{D}\cdot\sin(\omega t)]\boldsymbol{\varphi}, \tag{23}$$

where $\boldsymbol{\varphi} = (\varphi_{11}, \varphi_{12}, \cdots, \varphi_{1M_1}, \varphi_{21}, \varphi_{22}, \cdots, \varphi_{2M_2}, h)'$ and $\boldsymbol{M}, \boldsymbol{B}, \boldsymbol{C}, \boldsymbol{D}$ are constant matrixes whose elements are given in (15)–(22). It can be found that the equation (23) are ordinary differential equations with periodic coefficients. So the solutions can be obtained by Floquet theory.

According to Floquet theory[18], there exists a constant matrix $\boldsymbol{R}$ satisfies $\psi(t+T) = \boldsymbol{R}\cdot\psi(t)$, in which $T = 2\pi/\omega$, $\psi(t)$ is the fundamental solution matrix for system (23). If the eigenvalues of the matrix $\boldsymbol{R}$ are $\lambda_i (i = 1, \cdots, M_1+M_2+1)$, which are called Floquet multipliers, the solution of the linear system (23) can be written in the form of $\varphi_i = \mathrm{e}^{\gamma_i t} Z_i(t)$, where $\gamma_i = \frac{1}{T}\ln\lambda_i$, $Z_i(t)$ is a periodic function with a periods of $2\pi/\omega$, and γ_i are called as characteristic exponents.

In the present paper $\lambda_{\max}$ represents the largest modulus of all Floquet multipliers of fundamental solution matrix $\psi(T)$, and $\mathrm{Re}(\gamma)_{\max}$ is the growth rate of the most unstable mode, which corresponds to the real parts of characteristic exponent. The stability of system can be determined by $\lambda_{\max}$ or $\mathrm{Re}(\gamma)_{\max}$, If $\lambda_{\max} > 1$, namely $\mathrm{Re}(\gamma)_{\max} > 0$, the system is unstable; if $\lambda_{\max} < 1$, namely $\mathrm{Re}(\gamma)_{\max} < 0$, the system will be stable, if $\lambda_{\max} = 1$, namely $\mathrm{Re}(\gamma)_{\max} = 0$ the system is neutrally stable.

4 Floquet stability analysis

Based on the works of Zhou and Tang[12] who investigated the parametric resonance of inviscid liquid metal-gas jet with periodic fluctuation, and Wang, Hu and Zhou[13] who investigated the stability of two-layer flow with periodic fluctuation in a pipe, this study focus on the stability analysis of coaxial large density ratio viscous liquid-gas jet with periodic fluctuation. The physical parameters of liquid are based on liquid aluminum, and gas is nitrogen or argon. Thus $\rho_1 = 2500$ kg/m^3, $\mu_1 = 0.86 \times 10^{-3}$ Pa $\cdot$ s, $S = 0.836$ N/m; $\rho_2 = 0.5$ kg/m^3, $\mu_2 = 3.14 \times 10^{-5}$ Pa $\cdot$ s, The dimensionless parameters are given in the captions of figures presented, $\mathrm{Re}(\gamma)$ is growth rate of the system, k is wave number.

Varying the Weber number while keeping other parameters constant, Fig. 2 shows that there are three main unstable regions, they are the first one due to surface tension, the second one due to gas-liquid shear, and the third one with larger wave number due to velocity fluctuation. When Weber number is small, the unstable region caused by surface tension is dominated by the unstable region due to shear. Therefore the curves of $We = 7.3 \times 10^{-5}$ and $We = 1.0 \times 10^{-4}$ have only two unstable regions. As Weber number is increased, the unstable region due to shear becomes smaller and the growth rate decreases. It can be observed that the unstable region caused by surface tension appears in the curve of $We = 5.0 \times 10^{-4}$. So the effects of surface tension on the different unstable regions are quite different. Surface tension can cause instability, and it can suppress the instability due to shear, while it can hardly influence the instability caused by velocity fluctuation.

Figure 3 shows the effect of the viscosity of fluid with the stable and unstable regions in (k, Re) plane plotted. Because Reynolds number is inversely proportional to viscosity, the variation of Reynolds number will reflect the change of viscosity if other parameters are fixed. For small Reynolds number i.e. large viscosity, there is only one small unstable region. More and larger unstable regions appear with larger Reynolds numbers. It shows that the unstable regions dwindle and even disappear when the viscosity of fluid increase. So the viscosity of

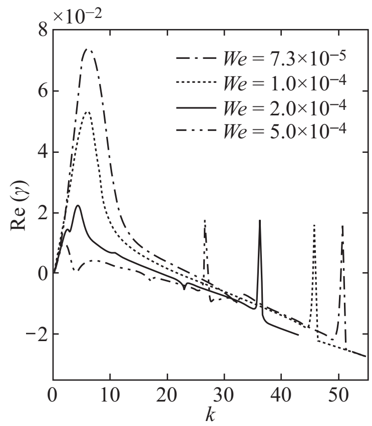

$Q = 2.0 \times 10^{-4}$, $N = 0.0366$, $\omega = 1$,
$Re = 1.9622 \times 10^5$, $Fr = 4.6492 \times 10^5$

Fig. 2 Effect of surface tension on stability

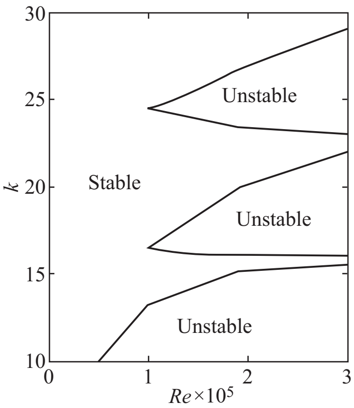

$Q = 2.0 \times 10^{-4}$, $N = 0.0366$, $\omega = 1$,
$We = 7.3394 \times 10^{-5}$, $Fr = 4.6492 \times 10^5$

Fig. 3 Effect of viscosity on stability

fluid suppresses the occurrence of the oscillating modes. When they investigated the parametric resonance of nonlinearly coupled micromechanical oscillators, Zhu and Ru[19] made the similar conclusion that the increasing damping is helpful to stabilize the system.

Figure 4 shows the effect of the velocity amplitudes on the stability. Zhou and Tang[12] found that when the velocity amplitudes is 0.1, there is obvious parametric resonance in the inviscid jet. For viscous jet with amplitude factor $Wc = 0.1$, only one unstable region is found with quite small growth rate. If increasing Wc to 0.5, two oscillating modes will appear in Fig. 4(a). When $Wc = 2$, the growth rate becomes larger and the unstable regions due to velocity fluctuation become evidently observable, as shown in Fig. 4(b). Along the wavenumber axis, the system goes through unstable–stable–unstable–stable–unstable–stable, which is a similar result with that of Zhou and Tang[12]. This concludes that the strength of velocity fluctuation enhances the parametric resonance of the system.

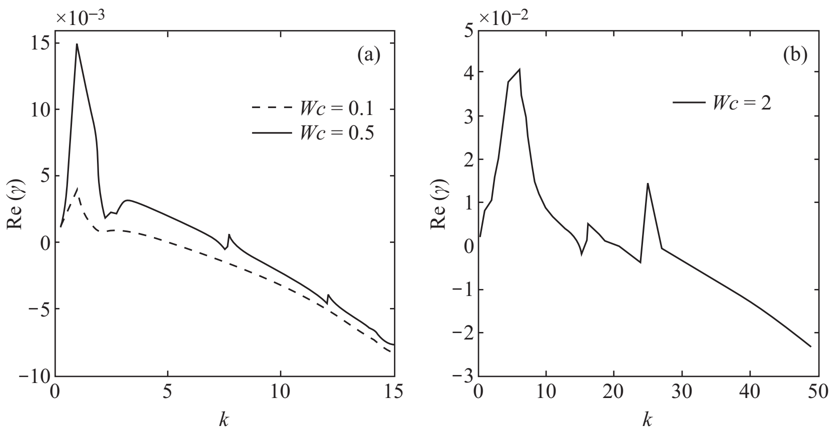

$Q = 2.0 \times 10^{-4}$, $N = 0.0366$, $\omega = 1$, $Re = 1.9622 \times 10^5$, $We = 7.3394 \times 10^{-5}$, $Fr = 4.6492 \times 10^5$

Fig. 4 Effect of Wc on growth rate

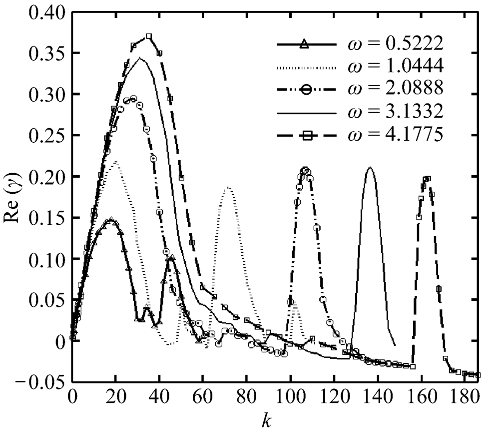

$Q = 6.9167 \times 10^{-4}$, $N = 0.0248$, $Re = 1.0213 \times 10^{6}$,
$We = 4.7493 \times 10^{-6}$, $Fr = 1.8710 \times 10^{6}$, $Wc = 0.7$

Fig. 5 Effect of frequency on stability

Figure 5 studies the influences of applied frequency on growth rate in $(k, \mathrm{Re}(\gamma))$ plane. As the frequency of velocity fluctuation increasing, the unstable region caused by fluctuation enlarges while the wave number of the most unstable wave increase, which implies that the diameter of breakup droplets will decrease. Zhou and Tang[12] and Wang, Hu and Zhou[13] also found that the increase of frequency will decrease diameter of breakup droplets, which is consistent with the present results.

The unstable region due to gas-liquid shear enlarges monotonously with the increase of frequency. Figure 6 shows that the growth rate of the most unstable wave due to shear increases monotonously. This is because the thickness of shear layer in unsteady flow decreases with the increase of frequency, as shown in Fig. 7.

To compare the theoretical results with the experiment of aluminum atomization by argon, which is conducted by Rai et al.[10,11,20] in USGA Process. Figure 8 shows the curves of stability analysis in $(k, \mathrm{Re}(\gamma))$ plane for three different experimental conditions, V_{g} is velocity of argon. Results indicate that: (i) The first unstable region with smaller wave-number is caused by

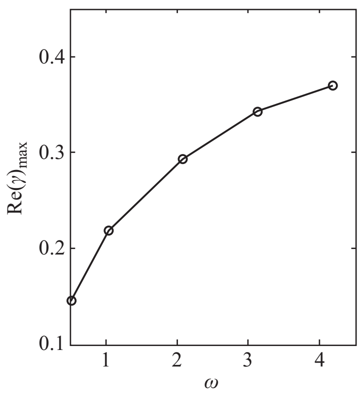

Fig. 6 Effect of frequency on Maximal growth rate $\mathrm{Re}(\gamma)$ due to shear

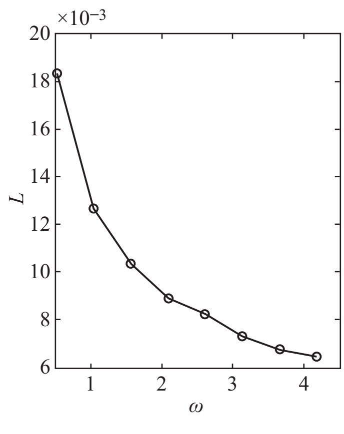

Fig. 7 Effect of frequency on thickness of shear layer L in unsteady flow

surface tension. As the velocity of argon is increased, its growth rate decreases. (ii) The liquid-gas shear or the velocity difference between gas and liquid will be helpful to enlarge the unstable region caused by shear. (iii) With the increase of gas velocity, the effect of the oscillation of argon become stronger, the unstable region duo to velocity fluctuation will become larger.

Although in most of cases we calculated the growth rate induced by shear is larger than that by fluctuation, it might be interesting to note that sometimes the later exceeds the former one, as shown in Fig. 2. Assuming the half wavelength of the most unstable wave is the average diameter of droplets, some results obtained are compared with the experimental data of Rai et al.[11] in Fig. 9. d_0 is the average powder size (sieved in microns), P_{gas} is atomizing gas pressure. It is found that the diameter of droplets in our result is in the same order of magnitude with experimental data and the tendency of variation of powder size agrees well with experimental data.

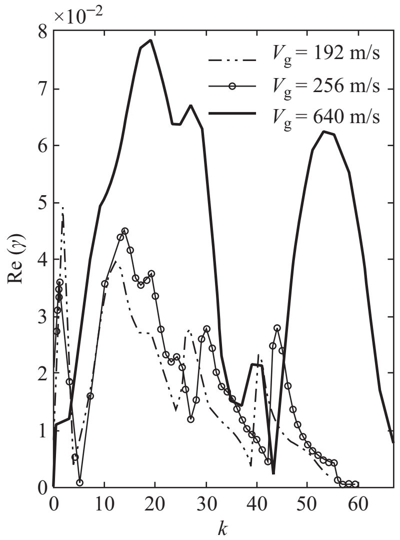

Fig. 8 Stability analysis of three experimental conditions

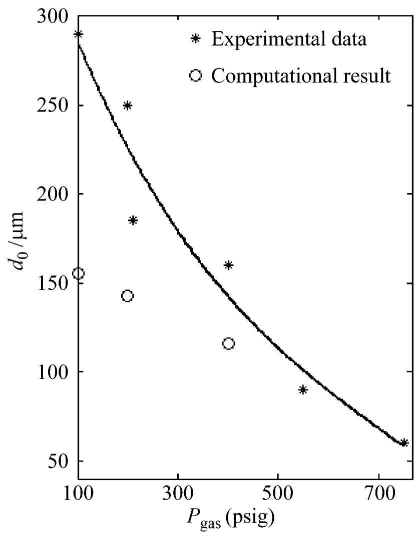

Fig. 9 Compare computational result with experimental data

5 Conclusions

The stability of a cylindrical viscous liquid metal jet in a coaxial viscous gas stream with periodic velocity fluctuation is investigated by Chebyshev collocation method and the Floquet theory. Since the exact solution with Bessel function for the unsteady basic flow is inaccurate when density ratio of liquid to gas is large, a Chebyshev collocation method is applied to solve the basic flow numerically. The effect of different physical parameters on the stability characteristics in liquid-gas jet are investigated in the present study. There are three possible unstable regions: the first one due to surface tension, the second one due to gas-liquid shear, and the third one with larger wave number due to velocity fluctuation.

Results show the amplitudes of velocity fluctuation have great impact on the stability of jet. The system becomes more unstable for larger amplitudes. The viscosity of fluid suppresses the occurrence of unstable mode induced by fluctuation. The unstable regions will dwindle, even disappear, with the increase of the viscosity of fluid. The surface tension of liquid hardly influences the instability which is caused by fluctuation, whereas affects the instability due to shear greatly. The frequency of velocity fluctuation has effect on both of the instability due to fluctuation and shear by changing the thickness of shear layer in unsteady basic flow. The enhancement of gas-liquid shear can decrease the unstable region due to surface tension, but increase the unstable region due to shear. Finally, the comparison of the present theoretical results of average diameter of droplets show qualitative agreement with the experimental data available.

References

[1] Plateau J. Statique experimentale et theorique des liquids soumle sux sseule forces[J]. *Moleculaire Gauthier Villars*, 1873, **1**(1):2–10.

[2] Rayleigh Lord. On the instability of jets[J]. *Proc London Math Soc*, 1879, **10**(1):4–13.

[3] Weber C Z. Zum zerfall eines flussigkeitsstrahles[J]. *Math Mech*, 1931, **11**(36):136–154.

[4] Chandrasekhar S. Hydrodynamic and hydromagnetic stability[M]. Oxford: Oxford University Press, 1961, p537.

[5] Keller J B, Rubinow S I, Tu Y O. Spatial instability of a jet[J]. *Phys Fluids*, 1973, **16**:2052–2055.

[6] Lin S P, Lian Z W. Mechnisms of the breakup of liquid jet[J]. *AIAA Journal*, 1990, **28**(1):120–126.

[7] Lin S P, Ibrahim E A. Instability of a viscous liquid jet surrounded by a viscous gas in a vertical pipe[J]. *J Fluid Mech*, 1990, **218**:641–58.

[8] Lin S P, Chen J N. Role played by the interfacial shear in the instability mechanism of a viscous liquid jet surrounded by a viscous gas in a pipe[J]. *J Fluid Mech*, 1998, **376**:37–51.

[9] Grant NJ. Rapid solidification of metallic particulates[J]. *Journal of Metals*, 1983, **35**(1):20–7.

[10] Rai G, Lavernia E J, Grant N J. Powder size and distribution in ultrasonic gas atomization[J]. *Journal of Metals*, 1985, **37**(8):22–26.

[11] Rai G, Lavernia E J, Grant N J. Effect of the atomisation variable on the powder characteristics in the USGA process[C]. In: *Proceedings of the Fifth International Powder Metallurgy Conference*, Princeton, N J, USA, 1986.

[12] Zhou Z W, Tang X D. The effect of the pulsation in gas flow on the stability of melted metal jet[C]. In: *Fourth International Conference on Spray Forming*, 1999.

[13] Wang Y X, Hu G H, Zhou Z W. Floquet stability analysis of two-layer flows in vertical pipe with periodic fluctuation[J]. *Applied Mathematics and Mechanics* (*English Edition*), 2006, **27**(8):1011–1019. DOI 10.1007/s10483-006-0801-1

[14] Woods D R, Lin S P. Instability of a liquid film flow over a vibrating inclined plane[J]. *J Fluid Mech*, 1995, **294**:391–407.

[15] Burya A G, Shkadov V Y. Stability of a liquid film flowing down an oscillating inclined surface[J]. *Fluid Dynamics*, 2001, **36**(5):671.

[16] Li X J, Hu G H, Zhou Z W. Variation of velocity profile of jet and its effect on interfacial stability[J]. *Applied Mathematics and Mechanics* (*English Edition*), 2005, **26**(1):1–6. DOI 10.1007/BF02438358

[17] Xinmin X. Numerical analysis of spectral method[M]. Beijing: Science Press, 2000 (in Chinese).

[18] He J, Wang Z. Ordinary differential equations[M]. Volume I, II, III. Hunan: Hunan Science and Technology Press, 1979 (in Chinese).

[19] Zhu J, Ru C Q, Mioduchowski A. High-order subharmonic parametric resonance of nonlinearly coupled micromechanical oscillators[J]. *Eur Phys J B*, 2007, **58**:411–421.

[20] Veistinen M K, Lavernia E J, Baram J C, Grant N J. Jet behavior in ultrasonic gas atomization[J]. *The International Journal of Powder Metallurgy*, 1989, **25**(2):89–92.